Received: 15 June 2021 | Revised: 12 November 2021 | Accepted: 12 November 2021

DOI: 10.1002/pen.25855

RESEARCH ARTICLE

POLYMER ENGINEERING AND SCIENCE WILEY

Control of end-of-life oxygen-containing groups accumulation in biopolyesters through introduction of crosslinked polysaccharide particles

Clelia Dispenza | Maria Antonietta Sabatino | Giulia Infurna | Nadka Tz. Dintcheva

Dipartimento di Ingegneria, Università di Palermo, Palermo

Correspondence
Nadka Tz. Dintcheva, Dipartimento di Ingegneria, Università di Palermo, Viale delle Scienze, Ed. 6, 90128 Palermo, Italy.
Email: nadka.dintcheva@unipa.it

Abstract

The formulation of bio-based materials with good performance in service and controlled end-of-life is imperative for an effective circular economy. In this work, an innovative approach to induce and control the end-of-life of biodegradable polyesters through introduction of crosslinked polysaccharide particles is proposed. Chitosan (Ch) has been subjected to ionotropically crosslinking and then added to polylactic acid (PLA) at different amounts (1.0–4.0%w) by melt mixing. All obtained results suggest that the addition of crosslinked Ch (cCh) particles does not modify significantly the investigated biopolyester properties. Specifically, the thermal analysis of the composites reveals that the addition of unmodified Ch alters the PLA thermal behavior, while the addition of cCh particles does not change the PLA glass transition, cold crystallization and fusion phenomena. The infrared and UV–visible spectroscopic analyses suggest no significant changes in PLA structure. PLA/cCh films show a good optical transparency, which is a desirable property for food packaging applications. In addition, thin PLA-based films have been subjected to UVB exposure and the accumulation of oxygen-containing groups has been monitored in time through spectroscopic analysis. Interestingly, at low exposure time, the presence of chitosan slows down the accumulation of these groups, while at long exposure time, chitosan induces accelerated oxygen-groups formation, supporting its beneficial effect as end-of-life accelerant.

KEYWORDS

ionotropically crosslinked chitosan, oxygen-containing groups accumulation, PLA photodegradation

1 | INTRODUCTION

The formulation of bio-based materials from naturally occurring sources is a very challenging issue, related to the gradual reduction of fossil-based sources, the development of a bio-based industry and the implementation of circular economy.[1,2] Although replacing of fossil-based polymers by biopolymers may have positive impacts on the environment and human health, the production of biopolymers at large

industrial scale and their end-of-life management are still challenging.[1,3–5]

Polylactic acid (PLA) is one of the most attractive biopolymers because of its compostability, biodegradability and properties that make it a good candidate in replacing fossil-based polyolefins for some industrial applications.[1,2,6–9] Therefore, the PLA shows inferior thermal and thermomechanical resistance with respect to synthetic polyolefins and to improve PLA poor properties, natural clay, metal oxides, natural fibers, cellulose, and so forth, have been evaluated as suitable additives.[6–11] These additives increase PLA thermal stability, hardness, and rigidity[12–16]; however, they reduce biodegradation rate.[12,17] PLA degradation depends on its molecular weight, macromolecular architecture, crystallinity degree, morphology, supramolecular structure, and so forth, but also on the surrounding environmental conditions such as moisture/water, oxygen content, pH, temperature, and/or kind and activity of microorganisms.[18–21] All degradation mechanisms, for example, hydrolytic, thermo-oxidative, photooxidative and biotic, have random chain scission as the first step. In addition, the thermal and photooxidative degradation chain scission occurs with simultaneous accumulation of oxygen-containing groups, and the latter facilitates further eventual polymer deterioration by microorganisms.[7,22,23]

The PLA degradation rate must be tailored to its specific application. However, different methods have been proposed currently to tailor the PLA degradation, including the incorporation of additives that increase the PLA hydrophilicity, and the incorporation of enzymes and/or other additives that decrease the activation energy of hydrolysis, and so forth Most of these methods are focused on modifying the hydrolytic rate or thermal degradation and only a few address the photodegradation.[24,25]

Chitosan is a cationic polysaccharide obtained by controlled NaOH deacetylation of chitin, which is a polysaccharide present in the exoskeleton of crustaceans, fungal cell walls and other biological materials.[26] Chitosan properties and performances depend on the deacetylation degree and the molecular mass.[27,28] When added as a filler to a polymeric matrix, chitosan can improve mechanical and barrier properties[29–32] because of its selectivity to CO_2 and O_2.[26,33]

In this work, ionotropically crosslinked chitosan (cCh) has been added to PLA at different amount (1.0–4.0%w) via melt mixing to induce and control PLA oxygen-containing group accumulation during exposure to UVB light, without detrimentally affecting the thermal and optical properties. The thermal behavior of PLA/cCh has been studied by differential scanning calorimetry and thermogravimetric analyses, alongside of PLA/Ch and neat PLA samples, for comparison. The morphology of all PLA-based films has been investigated by accurate scanning electron microscopy. Further, the optical transparency of PLA-based films has been evaluated by UV–vis spectroscopy, while the oxygen-containing group accumulation has been monitored in time through infrared spectroscopy.

2 | EXPERIMENTAL

2.1 | Materials

The materials used in this work are:

- PLA 3001D has been purchased from NatureWorks LLC. This material is an injection molding grade with melting point = 200°C; heat distortion temperature = 55°C; melt flow rate (210°C/2.16 kg) = 22; clarity–transparent.
- Low-molecular-weight chitosan with deacetylation degree in the range 75–85% and average molecular weight = 120 kDa, has been purchased from Sigma Aldrich.
- Glacial acetic acid, hydrogen chloride 37% (HCl), and disodium sulfate has been purchased from Sigma Aldrich.

2.2 | Preparation of ionotropically cCh microparticle/nanoparticle

In consideration of the large molecular weight distribution of the chitosan, the low-molecular-weight fraction was removed by dialysis. In particular, a 1% w/v aqueous solution of the polymer in 0.20% w/v acetic acid and 0.01 M HCl was prepared at room temperature by magnetic stirring for 24 h. The solution was then dialyzed against its own solvent (0.20% w/v acetic acid and 0.01 M HCl) for three 3 days using a 12 kDa cut-off dialysis membrane. The solution was then freeze-dried. After this treatment, a fraction corresponding to the 33.0 ± 4.0% of the total polymer was removed. The dry polymer was then redispersed in bi-distilled water containing 2.0%w acetic acid at 0.1 w/v, by magnetic stirring for 2 h. To a given volume of each solution a proper amount of 10% w/v disodium sulfate solution was added in order to keep the polymer to salt weight ratio always equal to 0.1. The addition was performed dropwise in an ultrasound bath at 25°C. After addition of the salt, the final mixture was sonicated for 10 min. The cCh particles were recovered by centrifugation at 13,000 rpm per 30 min at 15°C to remove the supernatant solution containing the excess of salt, redispersed in water and filtrated with 5 μm cut-off syringe filters to remove eventual larger aggregates and,

finally, dried in a vacuum oven at 40°C until constant weight was attained. No appreciable dry polymer weight change was measured.

2.3 | Processing by melt extrusion

PLA pellets were dried before processing for 24 h under vacuum in an oven at 70°C. The preparation of PLA-based samples was carried out using a HAAKE MiniLab Rheomex Micro-Compounder model CTW5 conical twin-screw extruder operating in a corotating mode. The processing temperature was 170°C, the residence time 5 min and the rotation speed was 100 rpm. Both untreated chitosan and cCh particles were added at 1.0% w and 1.0, 2.0, and 4.0%w, respectively, to the polymer melt after 2 min of processing. Neat PLA was subjected to the same processing condition.

Thin films (thickness about 60 μm) of neat PLA and PLA-based systems containing chitosan were obtained through compression molding (for 5 min at 6000 psi) in a Carver Laboratory Press.

2.4 | Characterizations

2.4.1 | Differential scanning calorimetry

The calorimetric data were evaluated by differential scanning calorimetry (DSC) using a PerkinElmer DSC7 calorimeter. All experiments were performed under dry N_2 on samples of around 10 mg in 40 μl sealed aluminum pans. Four calorimetric (two heating: 30–200°C and two cooling: 200–30°C) scans were performed for each sample at scanning heating/cooling rate of 10°C/min.

Crystalline degree has been calculated using the formula:

$$\chi_c = (\Delta H_f - \Delta H_{cc})/\Delta H^{o}{}_{f\,100\%\text{cryst PLA}}$$

where ΔH_f and ΔH_{cc} are the fusion enthalpy and the enthalpy of cold crystallization, respectively, and $\Delta H^{o}{}_f$ is the fusion enthalpy of 100% crystalline PLA (93.7 J/g).[34]

2.4.2 | Thermogravimetric analysis

Thermogravimetric analysis (TGA) was conducted with STA6000 PerkinElmer apparatus. Samples were tested in a temperature range of 30–600°C at a heating rate of 10°C/min under nitrogen flux (20 ml/min). The characteristic temperatures associated with the various phenomena are calculated as the peak temperature of the first derivative function (DTG).

2.4.3 | Scanning electron microscopy

Scanning electron microscopy (SEM) analysis was performed on cryogenically fractured and gold sputtered surfaces of thin films using a Philips (Netherlands) ESEM XL30 scanning electron microscope. The voltages used in SEM characterizations are 10.00 and 20.00 kV for observations of Ch particles and 10.00 and 30.0 kV for PLA-based systems.

2.4.4 | Fourier transform infrared analysis

A Fourier transform infrared (FTIR) spectrometer (Spectrum One, PerkinElmer) was used to record IR spectra using 16 scans at a resolution of 1 cm^{-1}. Measurements were obtained from the average of triplicate samples with a calculated maximum experimental error (relative standard deviation) of around 5%.

The progress of degradation for PLA and PLA-based systems has been followed by running FTIR analysis with time and monitoring the variations in the range 1800–1700 cm^{-1} in time, using Spectrum One software.

2.4.5 | UV–visible analysis

UV–visible (UV–vis) spectrometer, (Specord250 Plus, Analytik Jena), was used to record UV–vis spectra performing eight scans between 200 and 1100 nm at a resolution of 1 nm.

2.5 | Photooxidation exposure

Photooxidation tests of PLA and PLA-based films (thickness about 60 μm) were carried out using a Q-UV/basic weatherometer (from Q-LAB) equipped with UVB lamps (313 nm). The weathering conditions were a continuous light irradiation at $T = 55$°C. The progress of photooxidative degradation was followed by FTIR spectroscopic technique.

3 | RESULTS AND DISCUSSION

3.1 | Ionotropically cCh

Sodium sulfate was added to a diluted chitosan/acetate aqueous solution to prepare a cCh derivative using sulfate anions as ionic crosslinking points. The effect of ionotropic gelation on the thermal resistance of chitosan was investigated by TGA. The obtained thermograms are

plotted in Figure 1(A). Both Ch and cCh samples were dried for 24 h at temperature of about 80°C in a vacuum oven before the analysis. In the thermogram of Ch, a first weight loss of about 5%w is observed in the temperature range between 50 and 100°C, mainly due to the removal of bound water. The dehydration treatment, carried out before analysis, removed only plasticizing (unbound) water, that is, the free water present between polymer chains or very weakly bound water. This treatment did not remove adsorbed bound water, that is, water that is physically or chemically interacting with polymer chains, acetate ions and/or trapped in the crystalline domains.[35] The untreated chitosan is thermally stable up to about 250°C. The main pyrolytic degradation process of Ch takes place between 250 and 300°C with a relative steep weight loss (ca. 40%). The random split of the glycosidic bonds is accompanied by the release of low-molecular-weight compounds (H_2O, NH_3, CO, CO_2, and CH_3COOH) and significant structural rearrangements of the polymer chain segments (decomposition of pyranose rings through dehydration and deamination first and then ring-opening reactions). At about 450°C, the thermogram curve slope changes, becoming much less steep and causing a further weight loss (ca. 40%) in the temperature range between 450 and 600°C. The overall residual weight is of about 36% at 600°C. This second step of the thermal degradation process is associated with CH_4 evolution and consequent formation of a graphite-like structure via dehydrogenation mechanism.[36]

The thermogram of cCh clearly shows that the sample possesses a lower amount of bound water. This behavior has been already observed for other ionically crosslinked polyelectrolytes characterized by a relatively high crosslinking density.[37] The lower amount of bond water in cCh can be ascribed to two main reasons: (i) the reduction of the number of hydrophilic groups available to establish direct interactions with water (some hydrophilic groups are engaged in ion–ion bonds with dissociated potassium sulfate ions) and (ii) the restricted mobility of some hydrophilic groups that are not involved in crosslinks. Moreover, the crosslinking can increase the portion of amorphous regions of the polymer, and the latter reduces the amount of bound water trapped in the crystalline regions. At the same time, this creates cavities inside the material, thus favoring the access of free unbound water. This water was probably successfully removed by the thermal treatment under vacuum. Another noticeable difference with respect to the thermogram of Ch is that weight loss associated with thermal degradation is anticipated to 200°C, but it is much less significant. Indeed, the final residual weight at 600°C is of about 77% that is much higher than for untreated Ch. The decomposition reactions that start at lower temperatures likely involve in loosing of network chain ends, while the crosslinked portions undergo progressive carbonization without significant fragmentation. According to literature,[38] it is worth noting that the main decomposition processes for chitosan are radical reactions that can also evolve toward radical–radical combination, hence crosslinking. A small portion of the residual weight at 600°C can be attributed to the presence of the salt. In conclusion, the ionotropic crosslinking of chitosan has the advantage of reducing the amount of bound water, in comparison to the untreated chitosan, and this can mitigate the hydrolytic degradation of the host PLA matrix during melt processing at high temperature.

Figure 2(A–D) shows the scanning electron micrographs of cCh freeze-dried powder. The powder is rather

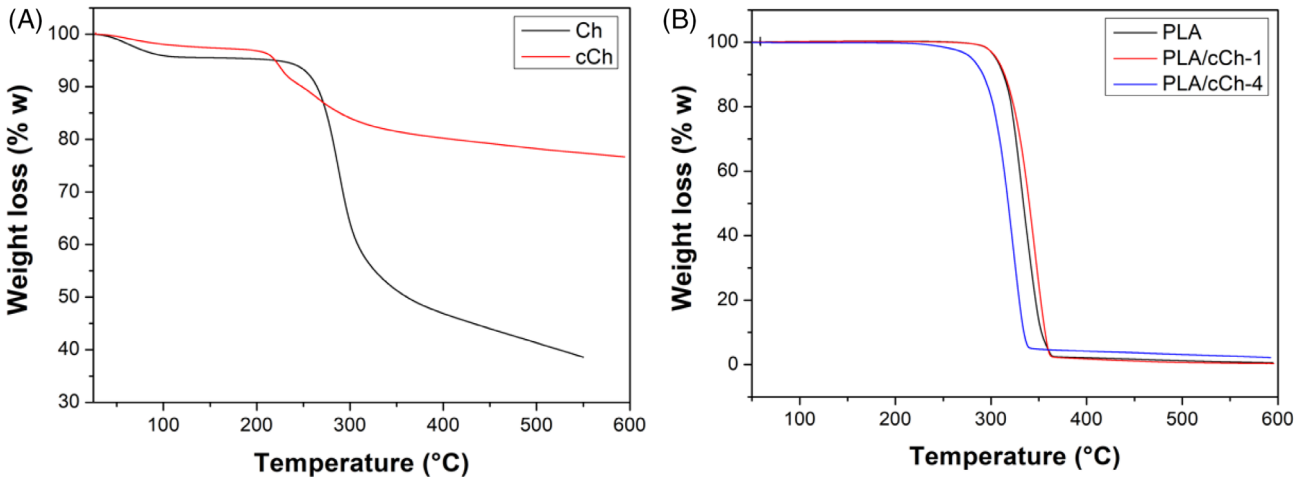

FIGURE 1 Thermogravimetric analysis (TGA) curves of (a) untreated chitosan, Ch, and crosslinked chitosan, cCh and (B) neat polylactic acid (PLA) and PLA containing crosslinked chitosan at different concentrations

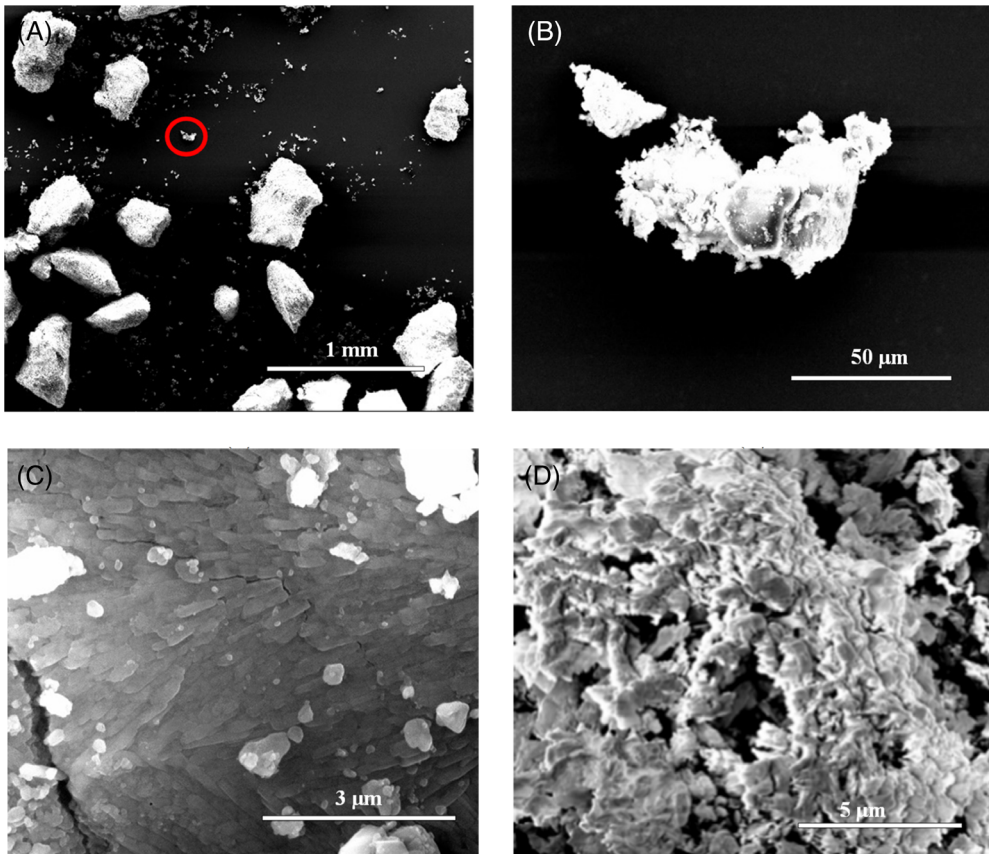

FIGURE 2 Scanning electron microscopy (SEM) micrographs at different magnifications of crosslinked chitosan

heterogeneous in size, showing small individual particles and large aggregates of hundreds of micrometers. At higher magnification, the larger particles appear like aggregates of nanoparticles with an elongated shape.

3.2 | PLA/ionotropically cCh composites

PLA-based systems containing 1.0%w untreated chitosan and 1.0, 2.0, and 4.0%w cCh were prepared by melt mixing and characterized for their morphological and thermal properties.

The morphology of the fracture surface of PLA/cCh composites was investigated by SEM, alongside with the fracture surfaces of PLA/Ch and neat PLA samples, for comparison. In Figure 3(A–I), representative micrographs are reported. The neat PLA sample shows smooth, laminated fractured surface (see Figure 3(A)) that confirm the well-known inherently stiff and brittle character of PLA. In Figure 3(B), the micrograph of PLA/Ch-1 composite is shown. The fractured surface morphology appears less smooth than for neat PLA. Several cracks and ridges are evident, which suggest that the chitosan has induced some ductile characteristics to PLA. In the micrographs of the PLA/cCh systems containing cCh concentration ranging from 1.0 to 4.0%w, can be observed a rougher fractured surface and an occasional presence of microparticles (10–30 μm diameter, (see Figure 3(C–E)). In particular, for PLA/cCh-4, there are large regions that appear homogeneous at lower magnification (Figure 3(F)) and much rarer zones with larger and irregular porous aggregates (Figure 3(G)). The apparently homogeneous regions, at higher magnification, show the presence of elongated nanoparticles (Figure 3(H,I)). It is also worth noting that the adhesion between the individual cCh microparticle/nanoparticle or their smaller clusters and the host matrix is rather good (see Figure 3(D,E, H,I)), indicating good compatibility between the biopolyester matrix and the more finely dispersed crosslinked polysaccharide particles.

In Figure 4, the second heating scans of different PLA-based samples containing untreated chitosan and cCh particles at different concentrations are plotted. In Table 1, all information extracted from the DSC curves shown in Figure 4, related to PLA glass transition (g), cold crystallization (cc), and fusion (f), are reported. The introduction of 1.0%w Ch leads to an anticipation of the glass transition phenomenon, for example, the onset temperature is slightly lower than the corresponding value for the neat PLA. Additionally, the presence of Ch causes the disappearance of the cold crystallization phenomenon and a significant reduction of the fusion enthalpy of the crystalline domains to

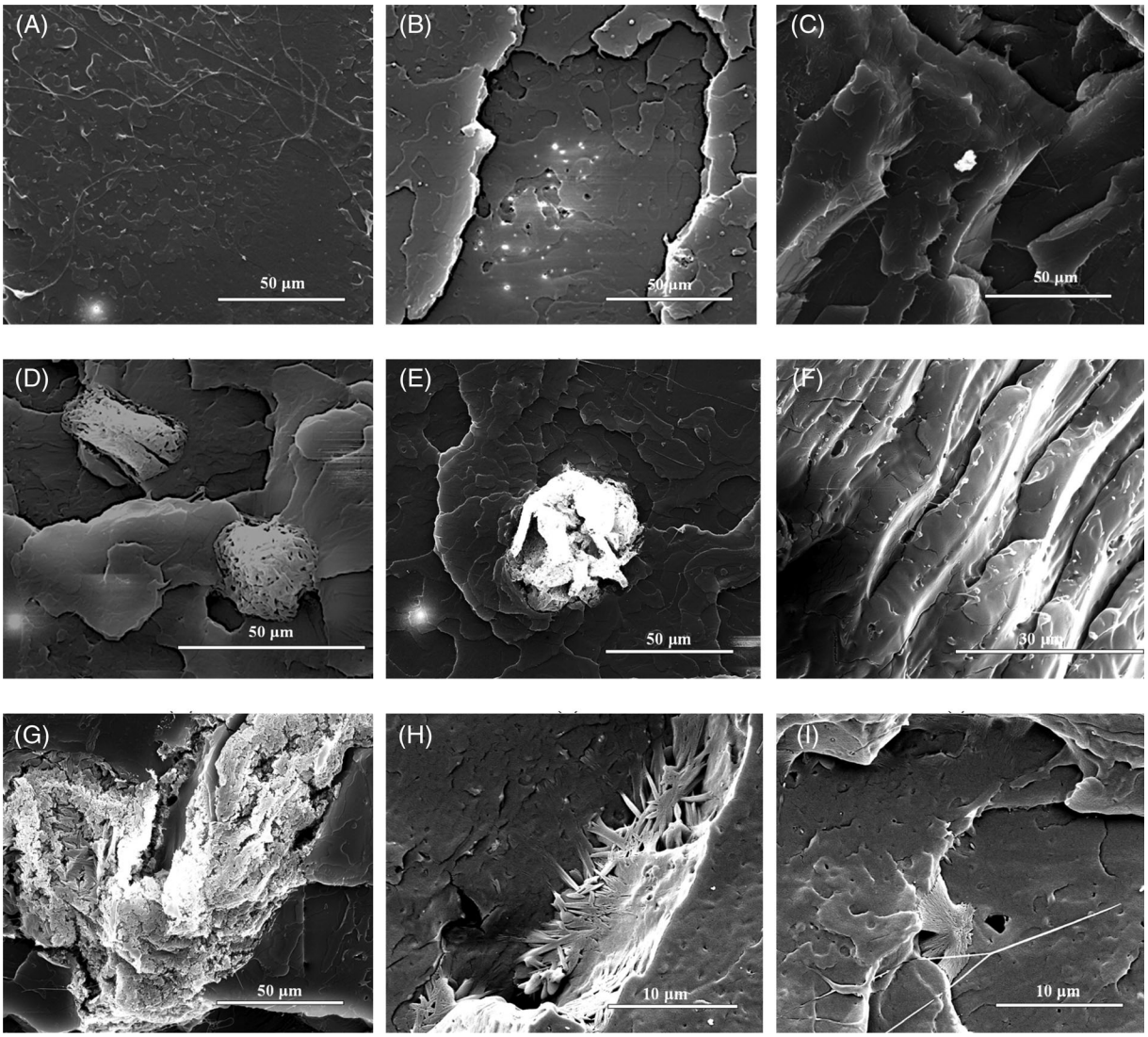

FIGURE 3 Scanning electron microscopy (SEM) micrographs of different polylactic acid (PLA)-based samples: (A) neat PLA; (B) PLA/Ch-1; (C) PLA/cCh-1; (D) PLA/cCh-2; and (E) PLA/cCh-4 (F,G). SEM micrographs of PLA/cCh-4 at higher magnification (H,I)

about 2.9 J/g, with respect to 43.7 J/g measured for neat PLA. This corresponds to a reduction of the crystalline degree from 5.1 to 3.1%. Contrarywise, the introduction of cCh in different amounts, that is, from 1.0 to 4.0%w, does not significantly influence the thermal transition phenomena (see Table 1). Indeed, the onset temperatures of the glass transition phenomenon remain almost unchanged and there are no major changes in the peak temperatures related to the cold crystallization and melting phenomena. The values of cold crystallization enthalpy are only 10% higher than those of neat PLA. The PLA/cCh-4 system shows a slightly increased crystalline degree, from 5.1 to 7.7%, probably because the cCh particles dispersed in PLA matrix act as nucleating centers.

The first fusion peak (T_{f1}), closely to the main fusion peak (T_{f2}), can be attributed to the melting of imperfect crystals. Indeed, during melt processing the PLA undergone thermomechanical degradation, generating PLA chains with low molecular weight that involve in imperfect crystals.[39] Interestingly, it can be also observed that this first fusion peak is slightly reduced for PLA/cCh-4 in comparison to neat PLA.

Therefore, the presence of untreated chitosan in blend with PLA has a negative effect on the thermal behavior and, more specifically, on the PLA cold crystallization and melting phenomena, that are no longer exhibited by PLA/Ch-1 (see Figure 4). In agreement with this result, the PLA/Ch-1 exhibit a predominantly amorphous state that involves poorer barrier properties and thermal resistance. On the contrary, the presence of ionotropically cCh does not have any significant effect on PLA crystallinity, except for PLA/cCh-4, and probably no impact on the service temperature, as well as its mechanical properties.[40–42]

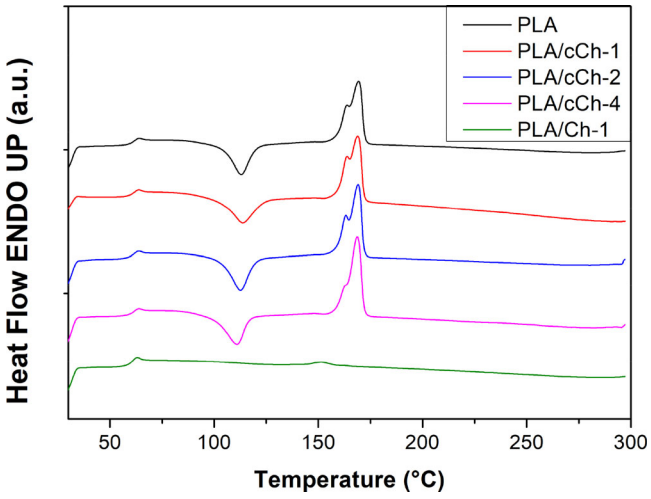

FIGURE 4 Differential scanning calorimetry (DSC) curves, second heating scan of neat polylactic acid (PLA), and PLA containing 1%w untreated chitosan (Ch) and 1.0, 2.0, and 4.0%w crosslinked chitosan (cCh)

The TGA of selected PLA-based systems, namely PLA/cCh1 and PLA/cCh4, was carried out under nitrogen atmosphere and the obtained thermograms are plotted in Figure 1(B). The thermogram of neat PLA is also reported for comparison. A single decomposition process can be seen for all systems. PLA thermal degradation is based on a hydroxyl end-initiated transesterification process and chain scission.[43] Various gaseous products, such as cyclic oligomers, lactide molecules, acetaldehyde, carbon monoxide, and carbon dioxide, are released during this process. The single decomposition temperature for both PLA/cCh systems points out a good compatibility between PLA and cCh. The onset decomposition temperature (T_d) is the same for neat PLA and PLA/cCh-1 and the mass loss at 600°C for both systems is around 99.5%. The presence of cCh at the highest concentration (4.0%w) causes a slight decrease of the degradation temperature and an increase of residual mass (ca. 2%). The decrease of degradation temperature for PLA/cCh-4,

TABLE 1 DSC data related to second heating scan of neat PLA and PLA-based samples containing untreated Ch and crosslinked chitosan microparticle/nanoparticle (cCh) at different concentrations

	Glass trans. (g)	Cold crystallization peak (cc)					Melt peak (f)				
Sample	T_{gonset} (°C)	$T_{cconset}$ (°C)	$T_{ccoffset}$ (°C)	T_{ccpeak} (°C)	ΔH_{cc} (J/g)	T_{fonset} (°C)	$T_{foffset}$ (°C)	$T_{f1\ peak1}$ (°C)	$T_{f2\ peak2}$ (°C)	ΔH_f (J/g)	X (%)
PLA	57.4	74.0	132.7	113.0	−38.9	148.0	181.8	163.7	169.3	43.7	5.1
PLA/Ch-1	57.0	-	-	-	-	134.6	172.4	151.5	163.4	2.9	3.1
PLA/cCh-1	57.6	71.5	133.4	113.7	−40.1	148.3	180.9	163.9	168.9	44.9	5.1
PLA/cCh-2	57.3	79.2	133.8	122.7	−42.6	148.1	178.4	163.2	169.0	47.4	5.1
PLA/cCh-4	57.9	77.6	132.7	110.8	−39.9	148.3	182.0	163.0	168.6	47.1	7.7

Abbreviations: Ch, chitosan; cCh, crosslinked Ch; DSC, differential scanning calorimetry; PLA, polylactic acid.

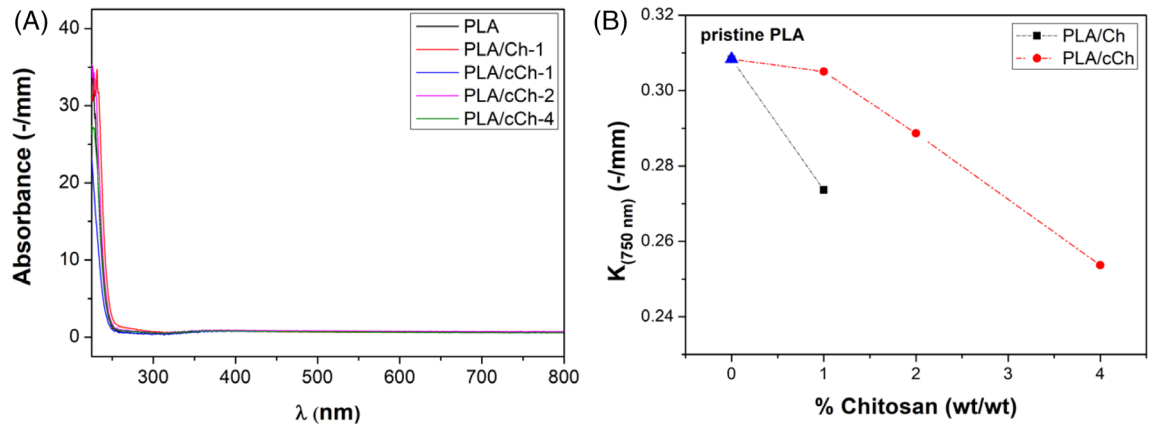

FIGURE 5 (A) UV–visible spectra of polylactic acid (PLA)-based samples containing chitosan (Ch) and crosslinked chitosan (cCh) and (B) linear attenuation coefficient, K, as a function of Ch concentration

despite of the observed slight increase of PLA crystallinity, can be related to the presence of cCh-based larger clusters in this system that, by creating heterogeneities, impact on the thermal stability of the composite material.

In Figure 5(A), the UV–vis of PLA-based samples containing Ch and cCh are plotted. The UV–vis spectra do not show any significant difference among PLA and PLA-based systems that contain Ch and cCh, highlighting no evident changes in the optical properties. The small differences in the UV adsorption, that is, in the 220–240 nm range, are nonsystematic and do not point to specific changes in materials structure. Additionally, to evaluate the film transparency, the linear attenuation coefficient (K) values were calculated considering the measured absorption values (A) at $\lambda = 750$ nm, samples thickness (D) and using the formula: $K = A/(2.3D)$.[44] The corresponding data are reported in Figure 5(B). Although the differences are small, the transparency of the PLA-based films is slightly lower due to the presence of both Ch and cCh. The K values decrease with increasing the cCh concentration and comparatively less with cCh than with Ch at the same concentration.

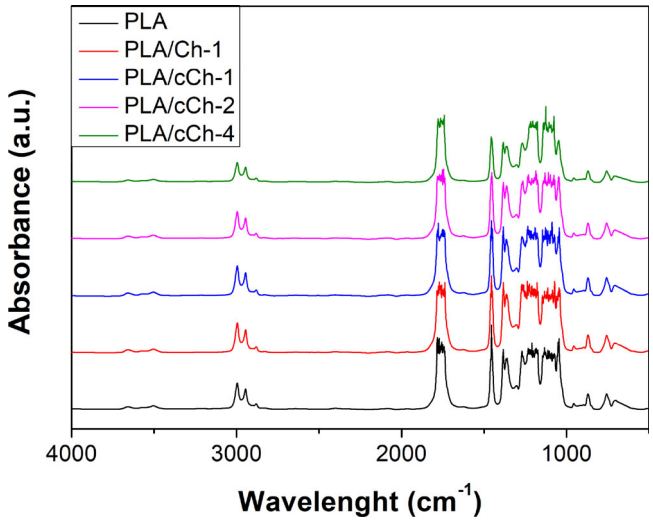

FIGURE 6 Fourier transform infrared analysis (FTIR) spectra of pristine polylactic acid (PLA) and PLA-based samples containing chitosan (Ch) and cCh

The chemical structure of PLA-based samples containing Ch and cCh was also investigated by FTIR analysis. In Figure 6, the FTIR spectra are reported, and in Table 2, the peak assignments for pristine PLA and Ch, also according to literature,[40] are noticed. The comparison among the various FTIR spectra does not reveal significant differences. This is mainly due to the similarity between PLA and Ch in terms of functional groups (carbonyl and methylene groups) and the relatively low amount of both Ch and cCh in the composites.

To sum up, the presence of cCh at 1.0, 2.0, and 4.0%w does not significantly modify the properties and performance of PLA, suggesting good compatibility between the matrix and cCh particles. The PLA/Ch, even if Ch is at a very low content, shows a lower crystallinity degree and inferior optical properties, that could compromise the application of PLA/Ch, for example, as food packaging material.

3.3 | Accumulation of oxygen-containing groups in PLA/Ch and PLA/cCh

To investigate the accumulation of oxygen-containing groups at end-of-life of PLA-based systems, the PLA/Ch

TABLE 2 Assignment of FTIR peaks for neat PLA[6] and neat chitosan[45]

PLA		Chitosan	
ν cm^{-1}	Attribution	ν cm^{-1}	Attribution
3500	—OH stretching (free)	2927	>C—H sym stretching
2993, 2879	>CH asym and sym stretching	1736	>C═O stretching
1748	—C═O carbonyl stretching	1626	C═O of secondary amide group (amide I)
1450	—CH_3 bending	1530	N—H bending (residue of amide II)
1382, 1357	>CH sym and asym bending	1395	C═N stretching (amide III band)
1259	—C═O bending	1353	N—H in plan deformation
1180, 1128	—C—O— stretching	955	Piranose ring
1083, 1043	—OH bending	890	C—N finger print band
954	—CH_3 rocking		
869, 756, 700	—C—C— stretching		

Abbreviations: FTIR, Fourier transform infrared analysis; PLA, polylactic acid.

and PLA/cCh thin films (thickness 60 μm) were subjected to accelerated UVB exposure. The accumulation of oxygen-containing groups, that could facilitate the PLA deterioration of microorganisms at its end-of-life, was monitored by FTIR analysis in time. All obtained FTIR spectra of PLA/Ch and PLA/cCh at 1.0, 2.0, and 4.0%w at different UVB exposure times, that is, from 0 to 960 h, are plotted as supplementary figures (see Figures S1(A)–S5(A)).

According to the literature, the PLA oxidation degradation mechanism occurs predominantly by random chain scission of the polymer backbone, and in Figure 7 (A),[46] main degradation mechanism is shown.[46] Besides, the oxidation of PLA in both melt state and solid state brings about a decrease of the PLA molar mass via pathway (1). The degradation pathways (2) and (3) would probably also occur, but the number of anhydrides species, possibly volatile, would be low and not detectable by FTIR. Therefore, the increase of the PLA absorption band, due to the presence of anhydride functions at around 1845 cm^{-1} and related to the accumulation of oxygen-containing groups, can be profitable followed by FTIR analysis.

As already pointed out, Ch degradation occurs mainly by depolymerization, that is, chain fragmentation, due to deacetylation and oxidation (see Figure 7(B)).[38]

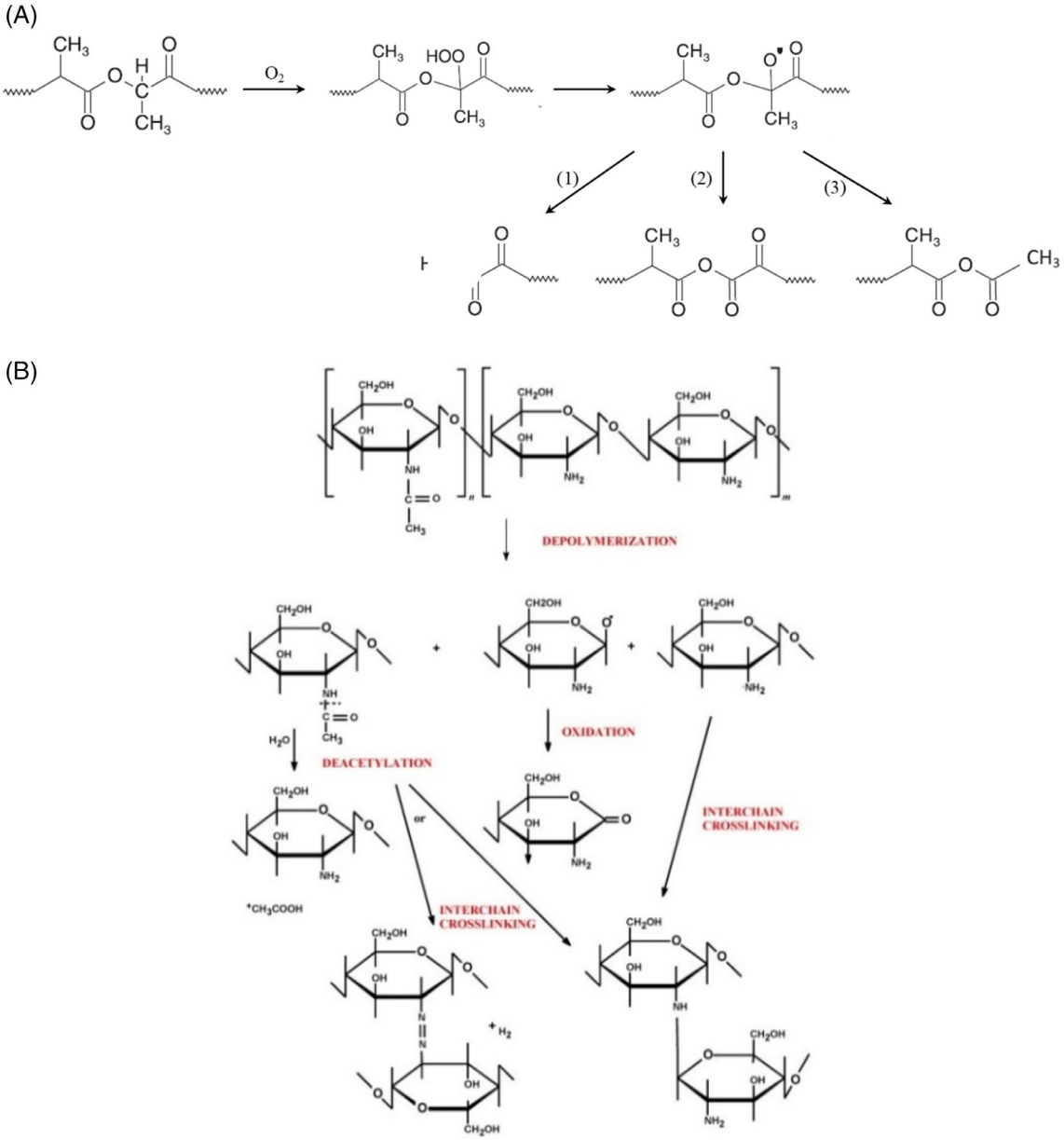

FIGURE 7 (A) Polylactic acid (PLA) oxidation mechanism, involving β-scission of alkoxy radical according to Reference [46]. (B) Chitosan degradation mechanism through depolymerization[38]

Furthermore, the new groups can react themselves, causing interchain crosslinking and 3D-structure formation.

As discussed above, the main FTIR absorption bands of PLA and Ch are overlapped, the detection of different peaks related to PLA or Ch degradation is very difficult, also considering that Ch and cCh are added at low concentration. Thus, to understand the photodegradation process, that is, accumulation of oxygen-containing groups, it is followed the variation of anhydride accumulations in PLA. In Figures S1(B)–S5(B) (supplementary figures), the carbonyl domains 1900–1500 cm^{-1}, that contains the PLA anhydride accumulations detectable at 1845 cm^{-1}, are plotted. In addition, in Figures S1(C)–S5(C) (supplementary figures), the subtracted spectra in the carbonyl domain, elaborated by FTIR software and calculated as $\Delta A_{(1845cm-1)} = A_{(t)} - A_{(0)}$, of PLA/Ch and PLA/cCh 1.0–4.0%w, are shown.

By means of subtracted spectra showed in Figures S1(C)–S5(C), it was possible to estimate the variations of anhydride accumulations for all investigated samples as a function of exposure time, and in Figure 8(A,B), obtained trends are plotted. At short exposure times, up to 400 h, the anhydride accumulation is more pronounced for neat PLA, rather than for PLA/Ch-1 (see Figure 8(A). Interestingly, at longer exposure times, up to 1000 h, the anhydride accumulation becomes more pronounced for PLA/Ch-1, in comparison to the neat PLA. As for the untreated chitosan, the addition of cCh particles at short exposure time slow down the anhydride accumulation of PLA, while at long exposure time results in accelerations of anhydride accumulation (see Figure 8(B). Specifically, the cross over between PLA and PLA/cCh-1.0, 2.0, and 4.0%w occurs, respectively, at 80, 170, and 260 h. Thus, the addition of cCh results in better pro-degradation action in comparison to blended chitosan. Moreover, it is worth noting that the trends of accumulation of anhydride functions increase with increasing the cCh concentration and this trend is particularly pronounced at longer exposure times for the higher concentration (see Figure 8(B). Probably at short exposure time, the radicals coming from chitosan depolymerization interact with the free radicals coming from β-scission of PLA. Over a certain time, that depends on chitosan concentration and chitosan chemical structure (untreated and cCh), the chitosan radicals accelerates the β-scission of PLA.

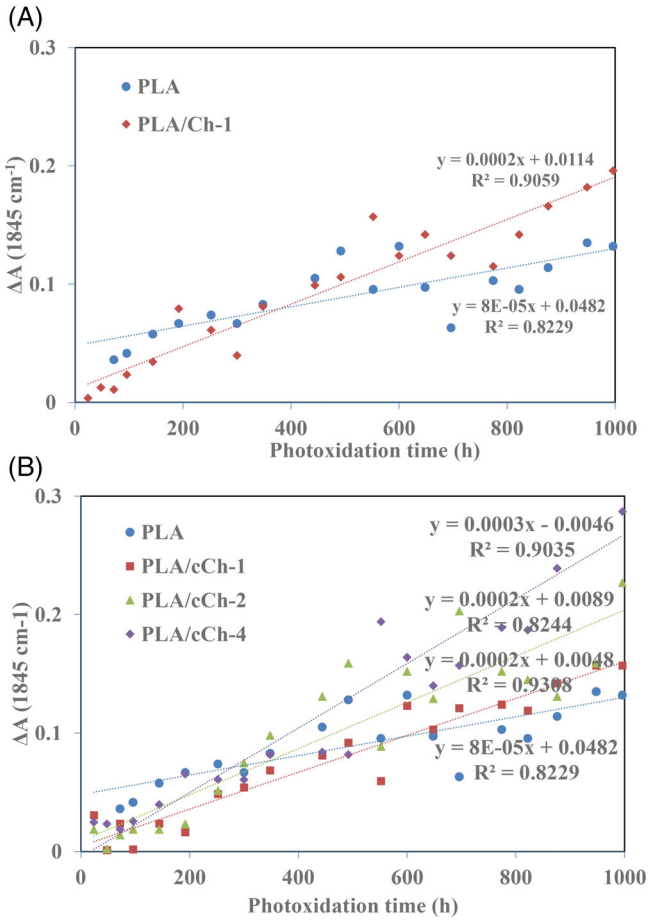

FIGURE 8 Analysis of anhydride accumulation as a function of UVB exposure time for polylactic acid (PLA)-based samples containing chitosan (Ch)

4 | CONCLUSIONS

An innovative sustainable approach to induce and control end-of-life oxygen-containing group accumulation in biopolyester, such as PLA, through introduction of polysaccharide particles, such as chitosan, is proposed. The chitosan has been subjected to ionotropically crosslinking to obtain microparticle/nanoparticles, and then, these particles have been introduced in PLA matrix through melt mixing at different concentrations (1.0–4.0%w). The cCh particles do not significantly modify the thermal behavior, spectroscopic properties, and morphology of PLA, while untreated chitosan, although added at low concentration, alters the PLA properties and performance.

To evaluate the oxygen-containing group accumulation, thin PLA, PLA/Ch, and PLA/cCh films have been subjected to accelerated UVB exposure and the accumulation of anhydride functions, coming from the PLA photodegradation, has been monitored through FTIR analysis in time. Obtained results suggests that at short exposure time, the anhydride accumulation is more pronounced for neat PLA, rather than for PLA/Ch and PLA/cCh, while at long exposure time, the pro-degradant effect of both Ch and cCh is well noticeable. Further, it is worth noting that the trends of accumulation of

anhydride functions increase with increasing the cCh concentration, suggesting a successful induction and control of the accumulation of oxygen-containing groups at PLA end-of-life.

ACKNOWLEDGMENT

Open Access Funding provided by Universita degli Studi di Palermo within the CRUI-CARE Agreement.

ORCID

Nadka Tz. Dintcheva https://orcid.org/0000-0003-3557-340X

REFERENCES

[1] M. Jamshidian, E. A. Tehrany, M. Imran, M. Jacquot, S. Desobry, *Compr. Rev. Food Sci. Food Saf.* **2010**, *9*, 552.
[2] L. T. Lim, R. Auras, M. Rubino, *Prog. Polym. Sci.* **2008**, *33*, 820.
[3] A. Di Bartolo, G. Infurna, N. T. Dintcheva, *Polymer* **2021**, *13*, 1229.
[4] I. Vroman, L. Tighzert, *Materials* **2009**, *2*, 307.
[5] P. Theinsathid, A. Chandrachai, S. Keeratipibul, *J. Technol. Manag. Innov.* **2009**, *4*, 82.
[6] G. H. Yew, A. M. Mohd Yusof, Z. A. Mohd Ishak, U. S. Ishiaku, *Polym. Degrad. Stab.* **2005**, *90*, 488.
[7] Y. Tokiwa, B. P. Calabia, *J. Polym. Environ.* **2007**, *15*, 259.
[8] X. Cai, H. Tong, X. Shen, W. Chen, J. Yan, J. Hu, *Acta Biomater.* **2009**, *5*, 2693.
[9] I. Panos, N. Acosta, A. Heras, *Curr. Drug Discov. Technol.* **2008**, *5*, 333.
[10] C. Zhang, L. Wan, H. Gu, Q. Hu, Y. Ding, S. Ying, *Polym. Eng. Sci.* **2021**, 1. https://doi.org/10.1002/pen.25819.
[11] H. Liu, B. Zhang, L. Zhou, J. Li, J. Zhang, X. Chen, S. Xu, H. He, *Polym. Eng. Sci.* **2021**, 1. https://doi.org/10.1002/pen.25812.
[12] A. R. McLauchlin, N. L. Thomas, *Polym. Degrad. Stab.* **2009**, *94*, 868.
[13] T. M. Wu, C. Y. Wu, *Polym. Degrad. Stab.* **2006**, *91*, 2198.
[14] H. M. C. d. Azeredo, *Food Res. Int.* **2009**, *42*, 1240.
[15] R. Nanda, A. Sasmal, P. L. Nayak, *Carbohydr. Polym.* **2011**, *83*, 988.
[16] K. Sungsanit, N. Kao, S. N. Bhattacharya, *Polym. Eng. Sci.* **2012**, *52*, 108.
[17] P. Chouwatat, P. Polsana, P. Noknoi, K. Siralertmukul, K. Srikulkit, *J. Met. Mater. Miner.* **2010**, *20*, 41.
[18] Y. Cheng, S. Deng, P. Chen, R. Ruan, *Front. Chem.* **2009**, *4*, 259.
[19] F. Tasaka, H. Miyazaki, Y. Ohya, T. Ouchi, *Macromolecules* **1999**, *32*, 6386.
[20] E. M. N. Polman, G. J. M. Gruter, J. R. Parsons, A. Tietema, *Sci. Total Environ.* **2021**, *753*, 141953.
[21] G. Kale, T. Kijchavengkul, R. Auras, M. Rubino, S. E. Selke, S. P. Singh, *Macromol. Biosci.* **2007**, *7*, 255.
[22] A. Sionkowska, A. Planecka, J. Kozlowska, J. Skopinska-Wisniewska, P. Los, *Carbohydr. Polym.* **2011**, *84*, 900.
[23] L. Zaidi, M. Kaci, S. Bruzaud, A. Bourmaud, Y. Grohens, *Polym. Degrad. Stab.* **2010**, *95*, 1751.
[24] S. Teixeira, K. M. Eblagon, F. Miranda, M. F. R. Pereira, J. L. Figueiredo, *C* **2021**, *7*, 42.
[25] N. F. Zaaba, M. Jaafar, *Polym. Eng. Sci.* **2020**, *60*, 2061.
[26] M. Z. Elsabee, E. S. Abdou, *Mater. Sci. Eng. C* **2013**, *33*, 1819.
[27] Z. Guo, R. Xing, S. Liu, Z. Zhong, X. Ji, L. Wang, P. Li, *Carbohydr. Polym.* **2008**, *71*, 694.
[28] H. K. S. Souza, J. M. Campiña, A. M. M. Sousa, F. Silva, M. P. Gonçalves, *Food Hydrocoll.* **2013**, *31*, 227.
[29] C. Branca, G. D'Angelo, C. Crupi, K. Khouzami, S. Rifici, G. Ruello, U. Wanderlingh, *Polymer* **2016**, *99*, 614.
[30] V. Epure, M. Griffon, E. Pollet, L. Avérous, *Carbohydr. Polym.* **2011**, *83*, 947.
[31] S. Sun, Y. Wang, L. Li, Z. Huang, H. Zhou, *Polymer* **2020**, *192*, 122335.
[32] Y. Yang, N. Yang, C. Zheng, Z. Shao, *Polym. Eng. Sci.* **2021**, 1. https://doi.org/10.1002/pen.25844.
[33] L. Sun, J. Sun, L. Chen, P. Niu, X. Yang, Y. Guo, *Carbohydr. Polym.* **2017**, *163*, 81.
[34] N. Najafi, M. C. Heuzey, P. J. Carreau, *Compos. Sci. Technol.* **2012**, *72*, 608.
[35] F. Wang, R. Zhang, T. Chen, P. Sun, *Polymer* **2016**, *8*, 149.
[36] J. Zawadzki, H. Kaczmarek, *Carbohydr. Polym.* **2010**, *80*, 394.
[37] Y. Yuan, Y. Huang, *Soft Matter* **2019**, *15*, 9871.
[38] E. Szymańska, K. Winnicka, *Mar. Drugs* **2015**, *13*, 1819.
[39] N. T. Dintcheva, S. Al-Malaika, E. Morici, R. Arrigo, *J. Appl. Polym. Sci.* **2017**, *134*, 1.
[40] R. Auras, B. Harte, S. Selke, *Macromol. Biosci.* **2004**, *4*, 835.
[41] B. Gupta, N. Revagade, J. Hilborn, *Prog. Polym. Sci.* **2007**, *32*, 455.
[42] A. Sodergard, M. Stolt, *Prog. Polym. Sci.* **2002**, *27*, 1123.
[43] H. Zou, C. Yi, L. Wang, H. Liu, W. Xu, *J. Therm. Anal. Calorim.* **2009**, *97*, 929.
[44] G. Infurna, G. Cavallaro, G. Lazzara, S. Milioto, N. T. Dintcheva, *Molecules* **2021**, *26*, 3468.
[45] M. Matet, M. C. Heuzey, E. Pollet, A. Ajji, L. Avérous, *Carbohydr. Polym.* **2013**, *95*, 241.
[46] N. T. Dintcheva, M. Baiamonte, M. Spera, *Polym. Degrad. Stab.* **2018**, *152*, 280.

SUPPORTING INFORMATION

Additional supporting information may be found in the online version of the article at the publisher's website.

How to cite this article: C. Dispenza, M. A. Sabatino, G. Infurna, N. T. Dintcheva, *Polym. Eng. Sci.* **2022**, *62*(2), 426. https://doi.org/10.1002/pen.25855